

Effect of seismic hazard definition on isolation-system displacements in nuclear power plants

Manish Kumar^{a,*} and Andrew S. Whittaker^b

^a Department of Civil Engineering, Indian Institute of Technology Gandhinagar, Gandhinagar, India, 382355; formerly graduate student at University at Buffalo, Buffalo, NY, 14260

^b MCEER and the Department of Civil, Structural and Environmental Engineering, University at Buffalo, Buffalo, NY, 14260

ABSTRACT

The effect of seismic hazard definition on the distribution of isolation-system displacements in a nuclear power plant (NPP) are studied in the paper and recommendations are made for design practice. The NPP is considered to be located at Diablo Canyon in California, a site of high seismic hazard, and is horizontally isolated using Friction Pendulum™ (FP) seismic isolation bearings.

Four descriptions of seismic hazard are investigated: uniform hazard response spectrum (UHRS), conditional mean spectrum (CMS), conditional spectra (CS), and UHRS-MaxMin. Uniform hazard response spectra are derived by probabilistic seismic hazard analysis and are the traditional description of seismic hazard in the nuclear industry in the United States. The UHRS is used to characterize the effects of design basis shaking but its ordinates across a wide range of period do not represent shaking associated with one ground motion set. The CMS and CS are derived from a UHRS and better characterize the effects of shaking from one ground motion set. The UHRS-MaxMin definition is also based on the UHRS but explicitly recognizes differences between motions in the orthogonal horizontal directions.

To investigate the utility of alternate descriptions of seismic hazard, the macro model of a seismically isolated NPP is subjected to ground motions consistent with the four definitions and for two intensities of earthquake shaking: design basis (DB) and beyond design basis (BDB) shaking as defined in the forthcoming seismic isolation NUREG. The coefficient of friction at the sliding surface is defined using two models: 1) Coulomb, and 2) p - T - v model that updates the coefficient of sliding friction at each time step as a function of axial pressure, temperature and sliding velocity.

The key results of the study, which are broadly applicable to sites of lower seismic hazard and other nonlinear bearings (e.g., the lead-rubber bearing), are: 1) the seismic hazard definition should account for differences between the amplitude of ground motions in the principal horizontal directions, 2) the displacement capacity of an NPP isolation system is controlled by the 90th percentile BDB shaking displacement, for a given hazard definition, and 3) the coefficient of friction at the sliding surface of a single-concave FP bearing should be defined using a p - T - v model because the standard Coulomb model may be inadequate for high values of axial pressure and nominal coefficient of sliding friction.

* Corresponding author.

E-mail address: mkumar@iitgn.ac.in (M. Kumar).

1. Introduction

Seismic isolation is a viable strategy for protecting safety-related nuclear structures, including nuclear power plants, from the effects of extreme earthquake shaking (e.g., Huang et al. [1], Kammerer et al. [2]). For large light water reactors, the isolation system will likely be installed in a horizontal plane, immediately below the basemat and above a foundation, as shown in Fig. 1. (For small modular and advanced reactors, isolators may be used to protect an entire plant but be placed at multiple levels below grade, or protect individual structures, systems and components within the plant; see [3] for details.) The performance of individual isolators is key to the response of a large light water reactor or similar, because a) individual isolator behaviors cannot yet be shown to be weakly correlated, requiring isolator behavior to be used to describe isolation-system behavior, and b) the isolation system is a singleton, with isolation-system failure potentially leading to core damage or large early release of radiation due to a cascading failure of containment. (Both assumptions are extremely conservative but will have to be proven on a project-specific basis. Isolator capacities may be strongly correlated but demands are likely weakly correlated: horizontal displacements may be similar but coexisting axial forces will vary widely, and isolators will be physically tested for maximum and minimum axial forces. Individual isolator failure will not result in either breach or collapse of the containment vessel: the basemat will be designed to span over multiple lost isolators per ASCE 4-16 [4] and the draft isolation NUREG [2], and pedestals will provide gravity support for the basemat in the event of isolator failure.)

The physical testing of prototype isolators will be required in US nuclear practice for axial force and lateral displacement demands consistent with extreme shaking: 90th percentile BDB displacements and the co-existing maximum/minimum axial forces. Assuming the probabilistic seismic hazard calculations are performed correctly, and nonlinear dynamic analysis is used to calculate demands on the isolated substructure, isolators and superstructure, it is important to generate consistent sets of ground motions as input to the analysis. Herein we study three representations of seismic hazard and two interpretations of geometric mean horizontal shaking. Single concave Friction Pendulum™ (FP) bearings are used to isolate the NPP but the results are directly applicable to other nonlinear isolation systems, including lead-rubber bearings and triple concave Friction Pendulum™ (FP) bearings.

Three representations of seismic hazard investigated are: uniform hazard response spectrum (UHRS), conditional mean spectrum (CMS), and conditional spectra (CS). The UHRS is the traditional measure of seismic hazard in the nuclear industry (e.g., [5]). The CMS is based on the UHRS, but has a spectral shape consistent with that of recorded ground motions (see [6]). Conditional spectra account for the variability in the ordinates of CMS at periods other than the conditioning period (e.g., [7]). Given a representation of the hazard (UHRS, CMS or CS), the spectra of the two orthogonal horizontal directions are typically assumed to be identical, even as the correlations between the acceleration histories in the two directions consistent with the spectra are rather weak (Huang et al. [8] note that the median, 90th percentile and 99th percentile correlations between the two recorded horizontal components are approximately 0.15, 0.30 and 0.50, respectively).

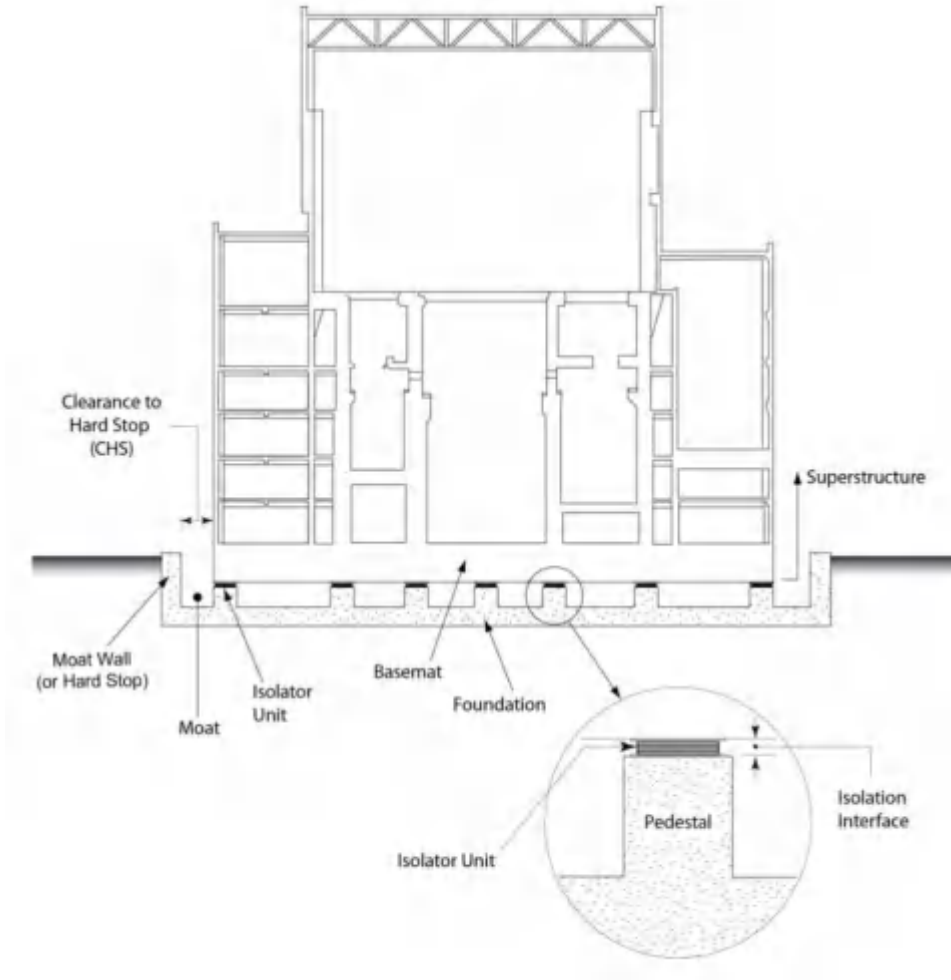


Fig. 1. A seismically isolated nuclear power plant (adopted from [2])

Two interpretations of a geometric mean horizontal spectrum are also considered, where the geometric mean ordinate at a specified period is equal to the square root of the product of the spectral accelerations at that period along the orthogonal horizontal axes: 1) both amplitudes are equal at a given period, and 2) the spectral amplitude of the shaking along one horizontal axis is greater (less) than the amplitude of the perpendicular component, UHRS-MaxMin (e.g., Huang et al. [9]), but their product, period-by-period, recovers the geometric mean horizontal spectrum.

As defined in the forthcoming NUREG [2], two levels of seismic hazard are considered for the analysis and risk assessment of base isolated nuclear power plants: ground motion response spectrum+ (GMRS+) and beyond design basis (BDB) GMRS. The two hazard levels correspond to the mean annual frequency of exceedance (MAFE) of 10^{-4} and 10^{-5} , respectively, provided that the GMRS+ spectrum exceeds the regulator-specific spectrum (see Kumar et al. [10]), which in the United States is typically a standard spectral shape anchored to a peak ground acceleration of 0.1 g.

The three hazard definitions and two ground motion interpretations are briefly discussed below. Sets of ground motions consistent with the UHRS, UHRS-MaxMin, CMS and CS, with MAFeS of 10^{-4} and 10^{-5} , are developed for the site of the Diablo Canyon Nuclear Generating Station (DCNGS) in California (latitude = 35.21162 N, longitude = 120.85562 W). The choice of hazard representation is investigated using calculated FP isolator displacements, estimated using a macro model of the isolation system as described by Kumar et al. [10]. The distributions of isolator displacement for a range of geometrical and material properties, and axial load, are computed and analyzed. Recommendations for design practice are proposed.

2. Descriptions of earthquake shaking in the orthogonal horizontal directions

The three representations of seismic hazard, namely, UHRS, CMS, and CS, and the interpretations of ground motion shaking are introduced below.

2.1. Uniform hazard response spectrum (UHRS)

The seismic hazard at a site of a nuclear power plant is typically described using a UHRS (see [11] for details). The UHRS is developed by probabilistic seismic hazard analysis (PSHA). The spectral ordinate at each period in the UHRS has the same probability of exceedance (e.g., 2%) in a specified time interval (e.g., 50 years). The UHRS accounts for the aleatory uncertainties in magnitude and location (source characteristics) of a possible earthquake, and in the intensity measure (IM, typically spectral acceleration) given the magnitude, location and other source properties. Different models (e.g., ground motion prediction equations) are used to quantify the source characteristics and IMs, because of uncertainties in the understanding of earthquake processes (e.g., type of faults, wave propagation characteristics). Such uncertainties are epistemic, which may be reduced as more data becomes available. These model uncertainties are generally accounted for using logic trees, each branch of which represents a model (e.g., a ground motion prediction equation) that is assigned a weight, based typically on engineering judgment. Finally, and period-by-period, the weighted spectral ordinates are added to construct the UHRS at a user-specified MAFe.

Fig. 2 shows the UHRS (solid line) for the DCNGS site corresponding to the hazard with a 2% probability of exceedance in 200 years (an MAFe of 1.01×10^{-4} or a return period of 9,900 years¹), obtained from <http://geohazards.usgs.gov/deaggint/2008/> on June 15, 2014, for the shear wave velocity in the upper 30 m of the soil column, v_{s30} , of 760 m/s: the boundary between Site Classes B and C per ASCE 7-10 [12]. The USGS website provides CMS for a user-specified conditioning period (also see Section 2.2), which is used to obtain the UHRS, noting that the UHRS ordinate at a given MAFe is equal to the corresponding CMS ordinate at the conditioning period T^* (see [6]).

¹ The hazard corresponding to MAFeS of 1.00×10^{-4} and 1.01×10^{-4} are not significantly different (see Kumar et al. [10]) and are assumed herein to be identical.

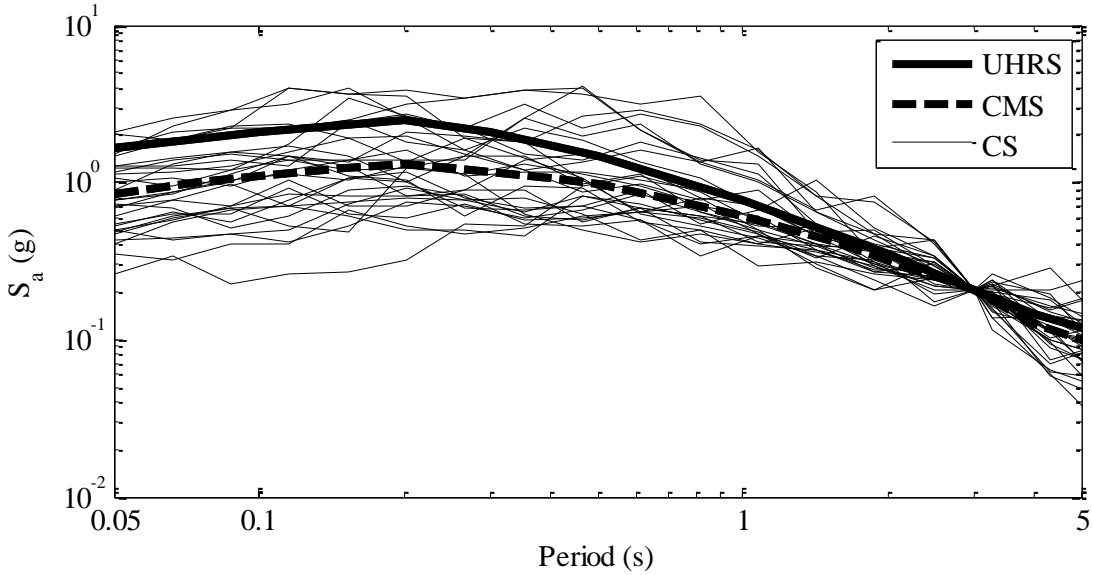


Fig. 2. Examples of a uniform hazard response spectrum (UHRS), and a conditional mean spectrum (CMS) and conditional spectra (CS) with the conditioning period of 3 s

2.2. Conditional mean spectrum (CMS)

Baker and Cornell [6] developed the conditional mean spectrum to better represent ground shaking associated with one earthquake record. The CMS has also been termed a scenario spectrum. The CMS is derived from a UHRS using a conditioning period and correlations between spectral accelerations at different periods, where the correlation coefficients are based on recorded ground motion data. The conditioning period is user specified and is commonly set equal to the first mode translational period (e.g., see [13]). The choice of conditioning period may not be clear if the structure is irregular, has significantly different first mode translational periods in the two orthogonal horizontal directions (e.g., [14]), is highly nonlinear, or is founded on compliant and nonlinear soils. At the conditioning period, the ordinate of the CMS is equal to that of the UHRS. The ordinates of the CMS of Fig. 2 (dashed line) are similar to those of the UHRS in the vicinity of the conditioning period (3 s). The CMS is obtained from the USGS website <http://geohazards.usgs.gov/deaggint/2008/>, accessed on June 15, 2014, using the GMPE of Campbell and Bozorgnia [15].

2.3. Conditional spectra (CS)

Conditional spectra (CS) address the randomness in the CMS ordinates given the spectral ordinate at the conditioning period (e.g., [7], [13]). Fig. 2 presents 30 CS with conditioning period of 3 s, representing the seismic hazard at the Diablo Canyon site with an MAE of 10^{-4} . The spectral ordinates of the UHRS, CMS and the 30 CS are equal at 3 s. Conditional spectra are calculated using software available at the Stanford University website http://web.stanford.edu/~bakerjw/gm_selection.html, accessed on June 15, 2014. This software uses the Campbell and Bozorgnia [15] GMPE to generate a set of CS. The (M, r, ε) triple at a period of 3 s is $(6.71, 5.5 \text{ km}, 1.92)$, corresponding to the Campbell and Bozorgnia [15] GMPE. The CMS from the USGS website (see Section 2.2) and the covariance matrix obtained using the

software written by the Baker Research Group are used to generate the 30 conditional spectra of Fig. 2.

2.4. *Ground motion interpretations: spectrum-consistent and MaxMin*

Traditionally, in the nuclear industry, the two orthogonal horizontal ground motions in a three-component set (including a vertical component) were scaled to a geometric mean horizontal spectrum: the UHRS. Variability in the amplitude of the two horizontal components was addressed, for the purpose of risk calculations, by increasing the dispersion in the plant-level fragility function: a reasonable approach if the soil beneath the plant could be treated as equivalent linear and the structures, systems and components comprising the plant responded to shaking in the linear range. A pair of seed horizontal motions, from a recorded set of three, would be scaled either loosely or tightly to the geometric mean horizontal spectrum. Tight matching to a geometric mean spectrum is generally accomplished using a time-domain, wavelet-based approach (e.g., [16], [17]). The correlation of the pair of scaled motions must be relatively small (see [4], [8]).

The two orthogonal horizontal components of recorded earthquake ground motions are consistently different (e.g., [1], [18], [19]) and the orientation of the maximum-direction shaking is random at a distance of more than approximately 5 km from the causative fault [20]. To accommodate this difference in the amplitude of the two horizontal components, a maximum-direction spectrum was developed and introduced into ASCE/SEI Standard 7-10 [12]. A uniform hazard response spectrum with maximum and minimum components (UHRS-MaxMin) accounts for the variability in the amplitude of shaking in the two orthogonal horizontal directions, in addition to the uncertainties considered in the development of UHRS. UHRS-MaxMin response spectra can be derived by amplitude scaling the UHRS, up and down, by a set of factors (e.g., [9]).

3. Seismic hazard in the vertical direction

Seismic hazard in the vertical direction can be calculated by PSHA using a GMPE developed using recorded vertical shaking data. Alternatively, the spectral ordinates in the vertical direction can be obtained by multiplying the horizontal spectral ordinates by period-dependent ratios of vertical-to-horizontal spectral acceleration (e.g., [21]). In this study, the NPP is subjected to the two horizontal components only because a) the vertical component does not materially change FP isolation-system displacements ([10], [22]), b) CMS and CS have not been extended to address vertical shaking, and c) the fundamental vertical period of an isolated nuclear structure will likely be a factor of 20+ times smaller than the fundamental horizontal period, making it difficult or impossible to select a defensible conditioning period.

4. 10,000-year response spectra

Ten thousand year return period UHRS, and CMS and 30 CS corresponding to conditioning periods of 2 s, 3 s and 4 s are generated for the Diablo Canyon site using the approach presented in Sections 2.1 through 2.3. Fig. 3(a) presents 5% damped UHRS, and CMS and CS in the horizontal direction corresponding to a conditioning period, T^* , of 2 s for the Diablo Canyon site and an MAFE of 10^{-4} . Figs. 3(b) and 3(c) present similar information for T^* of 3 s and 4 s,

respectively. Thirty pairs of UHRS-MaxMin spectra are generated by amplitude scaling the UHRS by the factors listed in Table 1 for the two orthogonal horizontal directions. The products of the factors for a given ground motion (GM) is one, namely, the geometric mean spectrum is recovered for each pair of ground motions. The maximum-direction multiplier of Direction X in the table has a median of 1.3 and a logarithmic standard deviation of 0.13 per Huang et al. ([9], [23]).

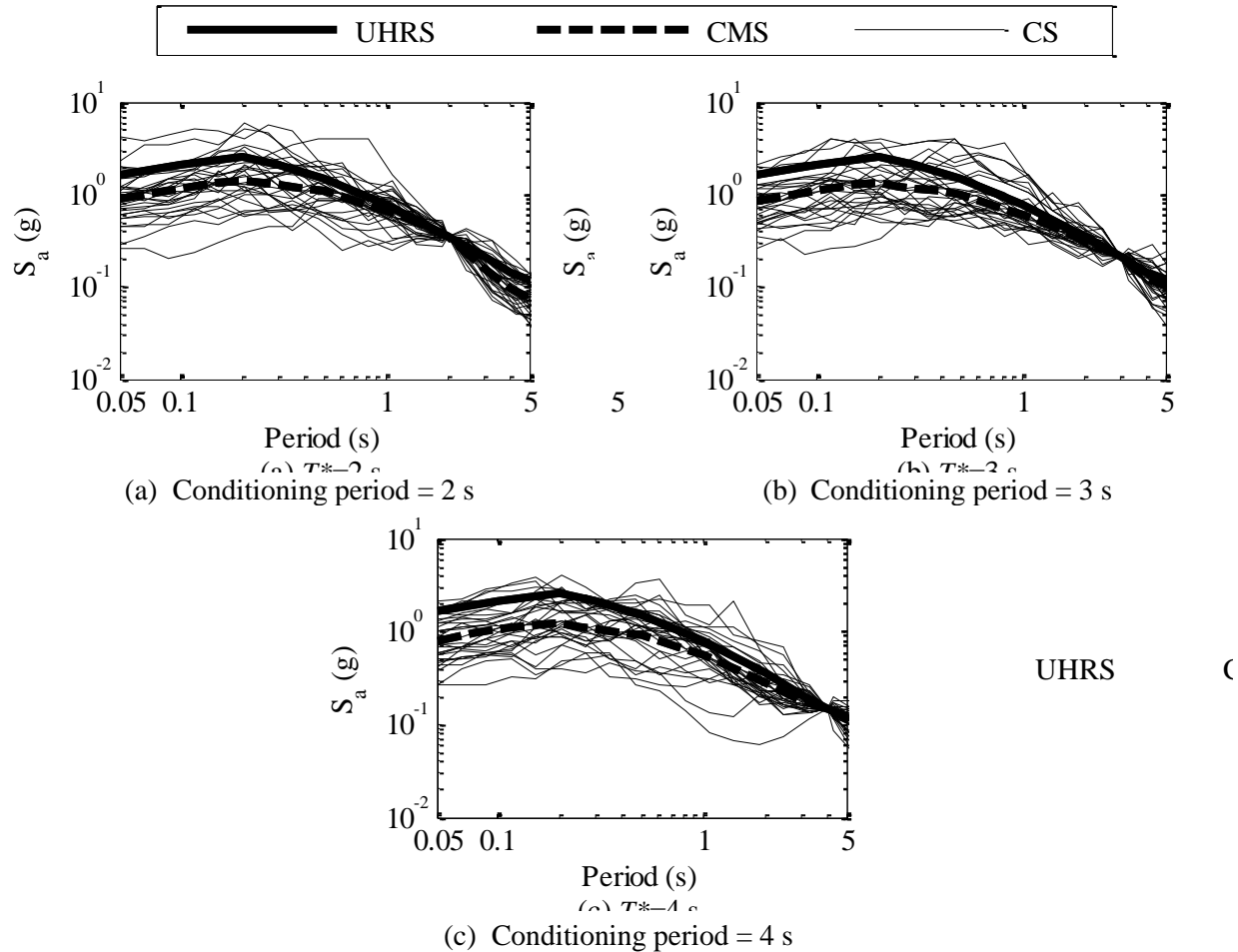


Fig. 3. Target uniform hazard spectrum (UHRS), and conditional mean spectrum (CMS) and conditional spectra (CS) with conditioning periods of 2 s, 3 s and 4 s for the Diablo Canyon site corresponding to a return period of 10,000 years

5. 100,000-year response spectra

Fig. 4 presents the UHRS for the Diablo Canyon site for return periods of 10,000 (Fig. 3) and 100,000 years (obtained from <http://geohazards.usgs.gov/hazardtool/application.php>, accessed June 15, 2014). The ratios of the spectral ordinates at the two return periods are between 2.0 and 2.2 over a period range of 0.5 s to 4 s. The 100,000-year UHRS is reasonably well calculated by multiplying the 10,000 year UHRS by 2.1. The UHRS-MaxMin spectra consistent with the

100,000-year hazard are also obtained by amplitude scaling the 10,000-year UHRS-MaxMin spectra² by a factor of 2.1.

Table 1. List of factors used to amplitude scale the ground motions spectrally matched to the UHRS

GM	Direction		GM	Direction		GM	Direction	
	X	Y		X	Y		X	Y
1	1.21	0.83	11	0.99	1.01	21	1.44	0.69
2	1.26	0.79	12	1.11	0.90	22	1.28	0.78
3	1.09	0.92	13	1.34	0.75	23	1.38	0.72
4	1.17	0.85	14	1.14	0.88	24	1.31	0.76
5	1.71	0.58	15	1.19	0.84	25	1.46	0.68
6	1.32	0.76	16	1.49	0.67	26	1.05	0.95
7	1.42	0.70	17	1.24	0.81	27	1.37	0.73
8	1.25	0.80	18	1.40	0.71	28	1.35	0.74
9	1.22	0.82	19	1.56	0.64	29	1.29	0.78
10	1.52	0.66	20	1.61	0.62	30	1.16	0.86

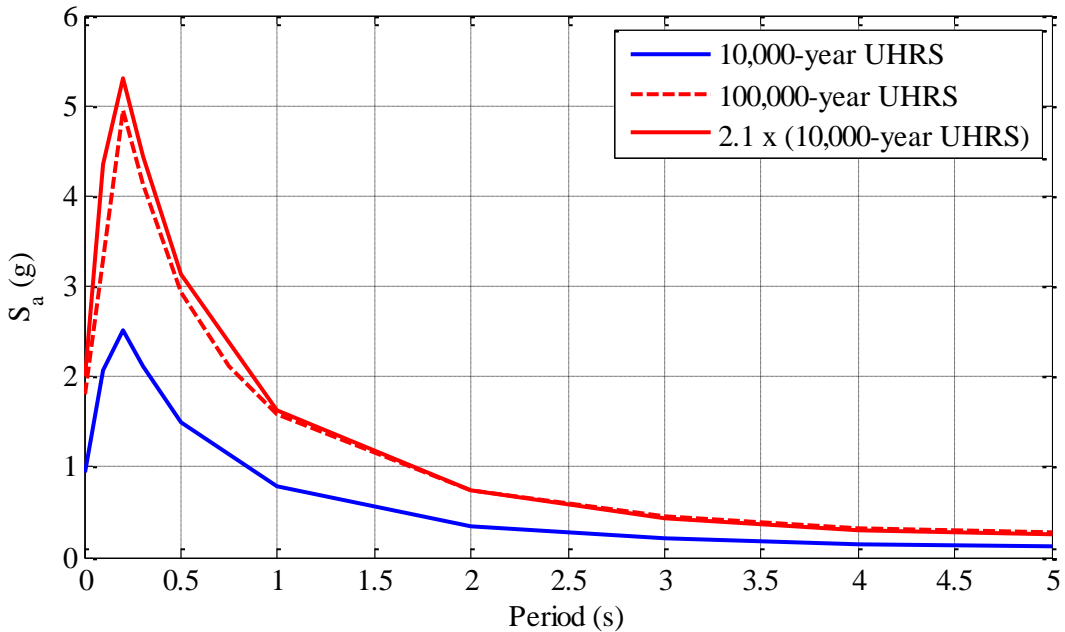


Fig. 4. 10,000- and 100,000-year return period UHRS for Diablo Canyon site

Figs. 5(a), 5(b) and 5(c) present the magnitude, source-to-site distance and ε , respectively, for a range of return periods and natural structural periods, corresponding to the Campbell and Bozorgnia [15] GMPE (data obtained from <http://geohazards.usgs.gov/deaggint/2008/>, June 15, 2014). The magnitude, distance and ε each trend to constant values at longer return periods. For a period of 2 s, the magnitude corresponding to 75-year return period is 6.19, which increases to 6.66 for a 10,000-year return period and to 6.72 for 20,000-year return period. The corresponding values for source-to-site distance are 34.7 km, 5.7 km and 4.8 km, respectively,

² The distributions of amplitude scaling factors in the two directions are assumed identical for the two return periods.

and for ε are 0.63, 1.88 and 2.02. Only ε changes appreciably at the longer return periods. Assuming that the magnitude and distance for a 100,000-year return period are equal to those for a 20,000-year return period (the greatest return period for which USGS data are available), the values of ε for 100,000-year hazard at periods of 2 s, 3 s and 4 s are 2.85, 2.91 and 2.84, respectively, which are considerably greater than the values of 2.02, 2.08 and 2.08, respectively, for a return period of 10,000 years.

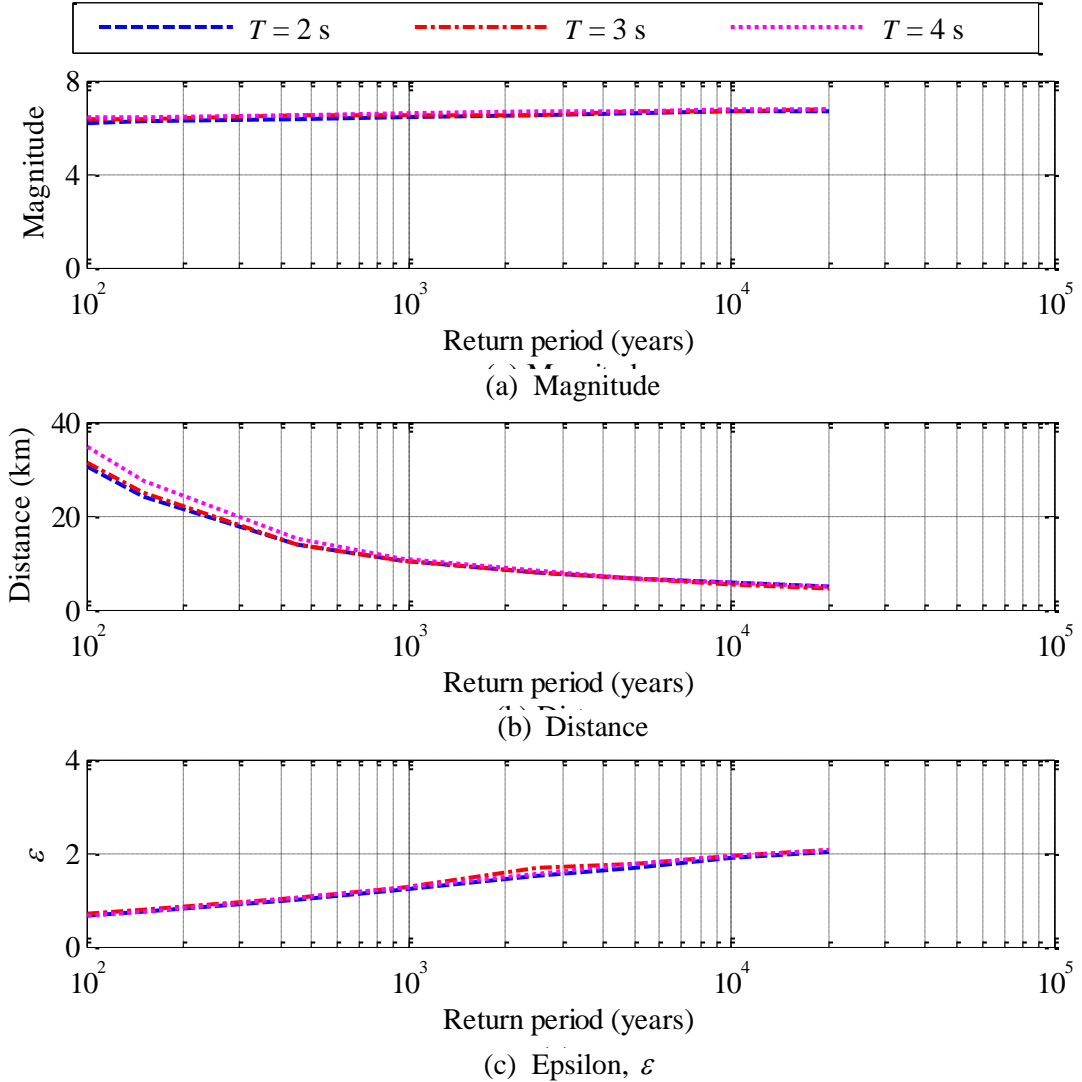


Fig. 5. Combinations of magnitude, source-to-site distance, and ε for the Diablo Canyon site

Conditional mean spectra with a conditioning period of 3 s are plotted in Fig. 6 for return periods of 10,000 and 20,000 years for the Diablo Canyon site. Also plotted in the figure is the 10,000-year CMS increased by a factor of 1.26. The spectral ordinate of the amplitude scaled 10,000-year CMS is equal to that for the 20,000-year CMS at the conditioning period, and is greater than that for the 20,000-year CMS at other periods. The shape of the CMS at a given conditioning period is a function of the hazard level and the shape of a CMS can be expected to

be sharper at the conditioning period at greater hazard levels: an attribute of positive epsilon motions identified by Baker and Cornell [6].

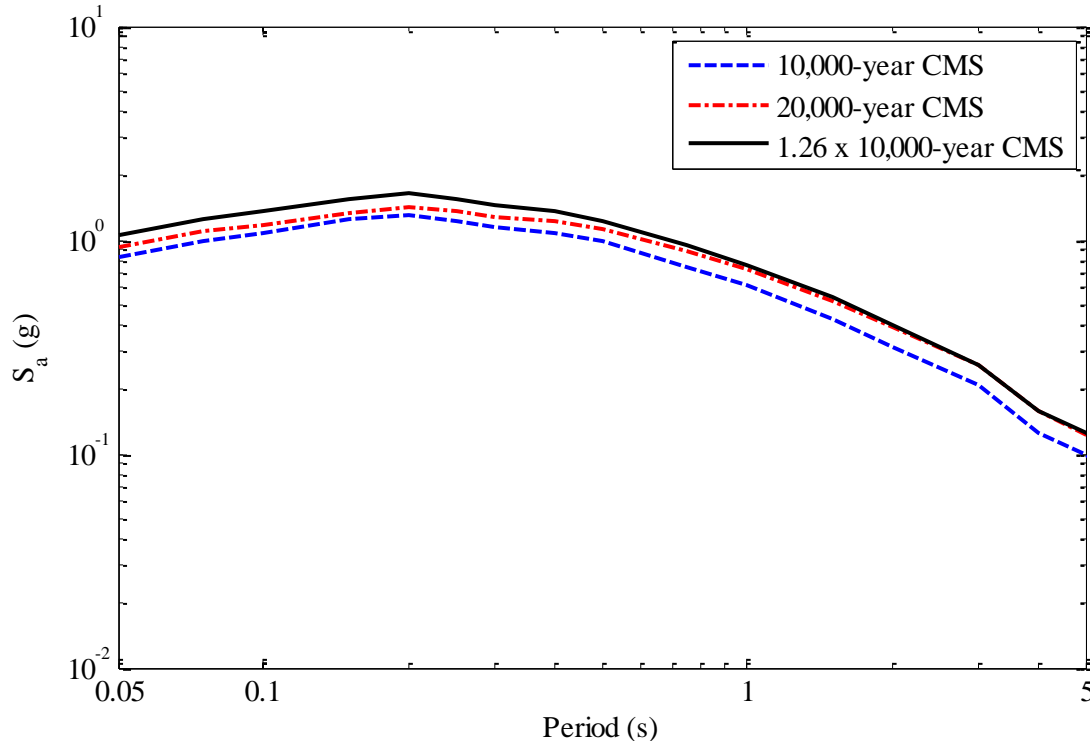


Fig. 6. Conditional mean spectra at the conditioning period of 3 s for seismic hazards with the return periods of 10,000 and 20,000 years

The USGS website does not provide CMS for a return period of 100,000 years. In this study, 100,000-year CMS are obtained by amplitude scaling the corresponding 10,000-year CMS by 2.1, which is a conservative representation of the seismic hazard (see for example Fig. 6) for periods other than the conditioning period.

As noted previously, CS account for variability in the CMS ordinates at periods other than the conditioning period. The variability is a function of the parameters of the earthquake (M and R) and the correlations between ε at different periods (see [7], [24]). The correlation coefficient between ε at two periods is a function only of the two periods and not of the values of ε at the two periods. Therefore, the distributions of the CS ordinates at periods other than the conditioning period are controlled by M and R but not ε . Since the disaggregated M and R are not considerably different for the 10,000-year and 100,000-year return periods (see Fig. 5), the covariance of the CS ordinates at different periods are expected to be comparable at the two hazard levels.

The information necessary to generate 100,000-year CS are not available on the USGS website. Noting that the shape of the CMS becomes sharper at the conditioning period as the return period is increased, and thus an increased ε given constant values of M and R , the CS obtained by amplitude scaling are likely conservative for the 100,000-year return period.

Accordingly, the 100,000-year CS are obtained by amplitude scaling the corresponding 10,000-year CS by a factor of 2.1.

6. Ground motions consistent with 10,000-year response spectra

6.1. Ground motions spectrally matched to UHRS

The set of 30 ground motions listed in Table E-1 of Kumar et al. [10] are scaled to match the 10,000-year UHRS of Fig. 4 in the period range of 0.5 s to 4 s using the software program RSPMatch [16]. The choice of period range is based on the following analysis.

The lateral force-displacement relationship for an FP bearing with a Coulomb-type coefficient of friction under constant axial load can be described by a bilinear relationship. The natural period before sliding, T_1 , is given by:

$$T_1 = 2\pi \sqrt{\frac{u_y}{\mu g}} \quad (1)$$

where u_y is the lateral displacement at which sliding begins, μ is the coefficient of sliding friction and g is the acceleration due to gravity.

The yield displacement can be taken as 0.001 m (e.g., [10]) and a representative coefficient of friction is 0.06 (0.1). The corresponding T_1 is 0.25 s (0.2 s), suggesting initially that the lower bound on the range should be 0.25 s. The sliding periods of the FP bearings considered in this study are no greater than 4 s, with effective periods, based on secant stiffness, of much less than 4 s if the displacement is small. The period range for spectral matching of 0.5 s to 4 s (and not 0.2 s to 4 s) is a compromise associated with the significant computational expense³ of decreasing the lower bound on the range from 0.5 s to 0.2 s. It is shown in Kumar et al. [10] that the value of the yield displacement (accordingly, the lower limit of the period range for scaling) does not considerably influence the isolation system displacement.

Fig. 7(a) presents the response spectra of the 30 seed ground motions of Table E-1 of Kumar et al. [10] spectrally matched to the UHRS in X direction. The target UHRS is also plotted in the panel. Fig. 7(b) presents companion information in the Y direction. The spectra of the matched motions are virtually identical to the target spectra in the two orthogonal horizontal directions. The maximum, minimum, and average values of the correlation coefficient of these scaled ground motions are 0.50, 0.00, and 0.20, respectively.

³ Spectrally matching a ground motion component to a randomly generated conditional spectrum (discussed later) can be computationally expensive if the period range is broad.

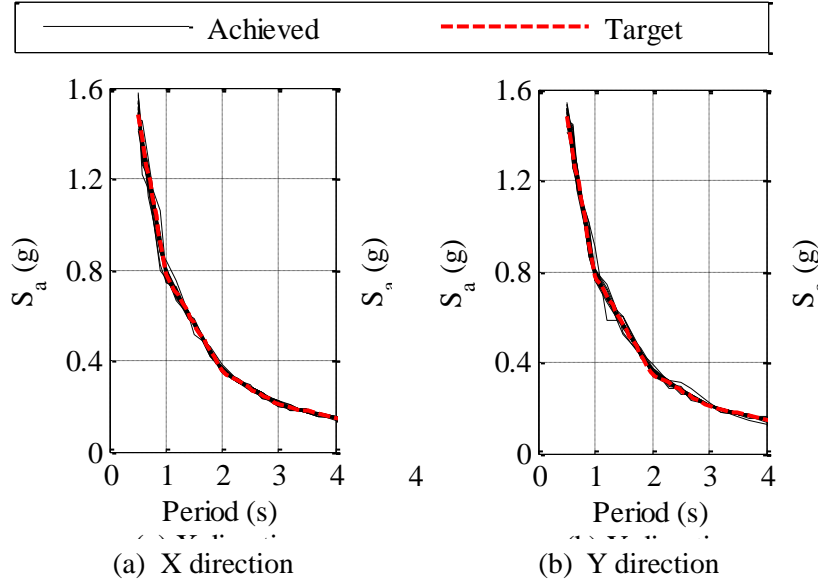


Fig. 7. Response spectra of 30 seed ground motions spectrally matched to the 10,000-year UHRS for the Diablo Canyon site

6.2. Ground motions consistent with UHRS-MaxMin

The response spectra of the scaled ground motions of Section 6.1 are identical in the two horizontal directions. The ground motions consistent with UHRS-MaxMin spectra are developed by amplitude scaling, up or down, the two horizontal components of the spectrally matched ground motions of Section 6.1. The scaling factors are listed in Table 1. Fig. 8 presents the response spectra of the ground motions consistent with UHRS-MaxMin.

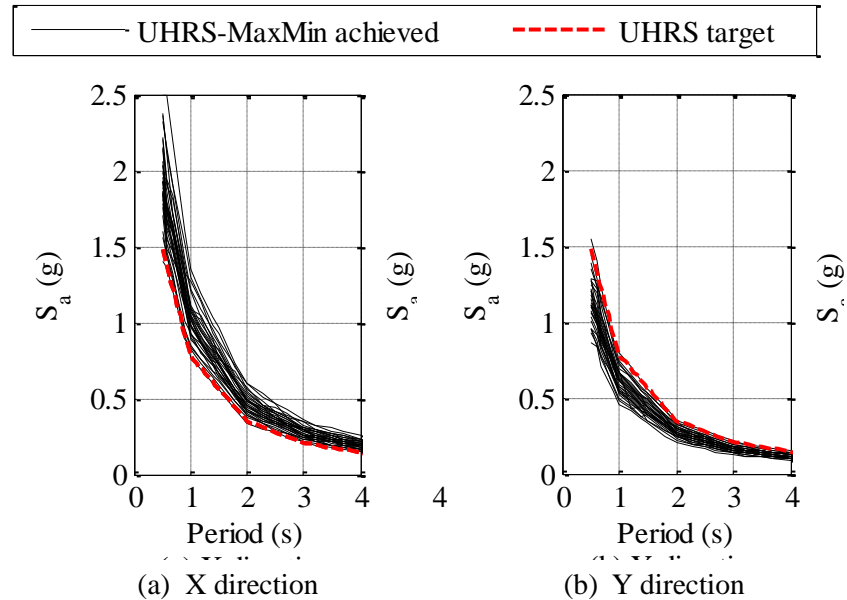


Fig. 8. Response spectra of 30 seed ground motions consistent with the 10,000-year UHRS-MaxMin for the Diablo Canyon site

6.3. Ground motions spectrally matched to CMS

Conditional mean spectra with conditioning periods of 2 s, 3 s and 4 s are used to represent 10,000-year seismic hazard at the Diablo Canyon site. The three CMS are plotted in Fig. 2. The 30 seed motions of Table E-2 of Kumar et al. [10] are spectrally matched to the three CMS, in the two horizontal directions, in the period range of 0.5 s to 4 s. Figs. 9(a), 9(b) and 9(c) present the target conditional mean spectrum with a conditioning period of 2 s, 3 s and 4 s, respectively. Also plotted in the three panels are the response spectra of the 30 matched motions in the X direction. The remaining three panels in the figure present identical information in the Y direction. The spectra of the matched motions are virtually identical to the target spectra. The maximum, minimum, and average values of the correlation coefficient of these scaled ground motions are approximately 0.40, 0.00, and 0.13, respectively.

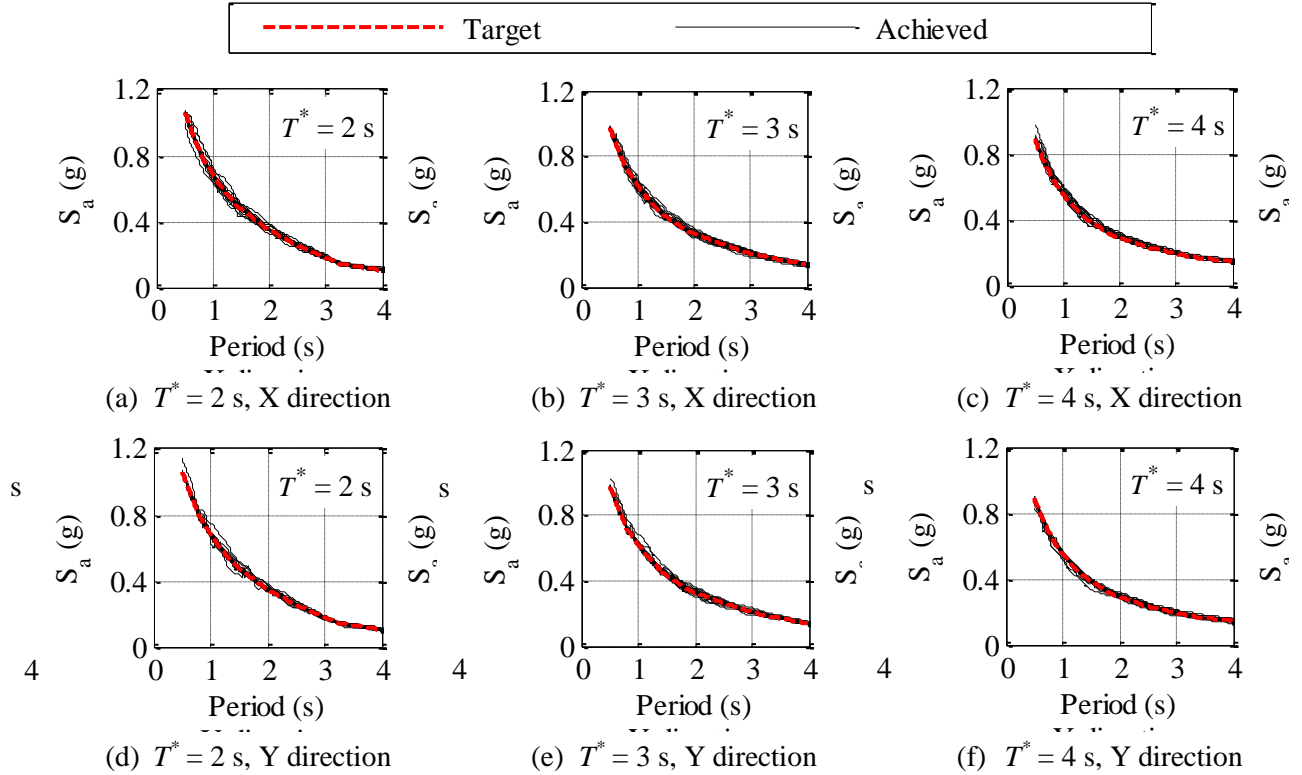


Fig. 9. Response spectra of 30 seed ground motions spectrally matched to the 10,000-year conditional mean spectra for the Diablo Canyon site

6.4. Ground motions spectrally matched to CS

A set of 30 conditional spectra is generated for each of the three conditioning periods, namely, 2 s, 3 s and 4 s (see Fig. 2): CS Set 1, CS Set 2 and CS Set 3. Three sets of 30 seed ground motions are used: GM Set 1, GM Set 2 and GM Set 3 (Tables E-3, E-4 and E-5 of Kumar et al. [10], respectively). The 30 ground motion records of GM Set 1 are matched to the 30 conditional spectra of CS Set 1 (each record scaled to one conditional spectrum). Similarly, the ground motions of GM Set 2 and GM Set 3 are matched to the spectra of CS Set 1. The three sets of seed ground motions are also matched to the other two sets of conditional spectra, CS Set 2

and CS Set 3. The end product of this exercise is three sets of ground motions matched to each of the three sets of conditional spectra – nine sets of 30 CS-scaled ground motions.

Fig. 10(a) presents the mean of the 30 target conditional spectra with the conditioning period of 2 s (Fig. 3(a)) and the mean of the computed spectra of the X component of the 30 ground motions for each of the three spectrally matched GM Sets. Fig. 10(b) presents the standard deviation in the target and computed spectra, noting that the value is zero at the conditioning period of 2 s. The remaining panels in the figure present the corresponding information for conditioning periods of 3 s and 4 s. The mean and standard deviation of the spectral ordinates of the scaled motions compare very well with the target values. More details on the CS-scaled motions are presented in Kumar et al. [10]. The correlation coefficients between the two horizontal components of these three sets of ground motions are generally consistent with the observations by Huang et al. [8].

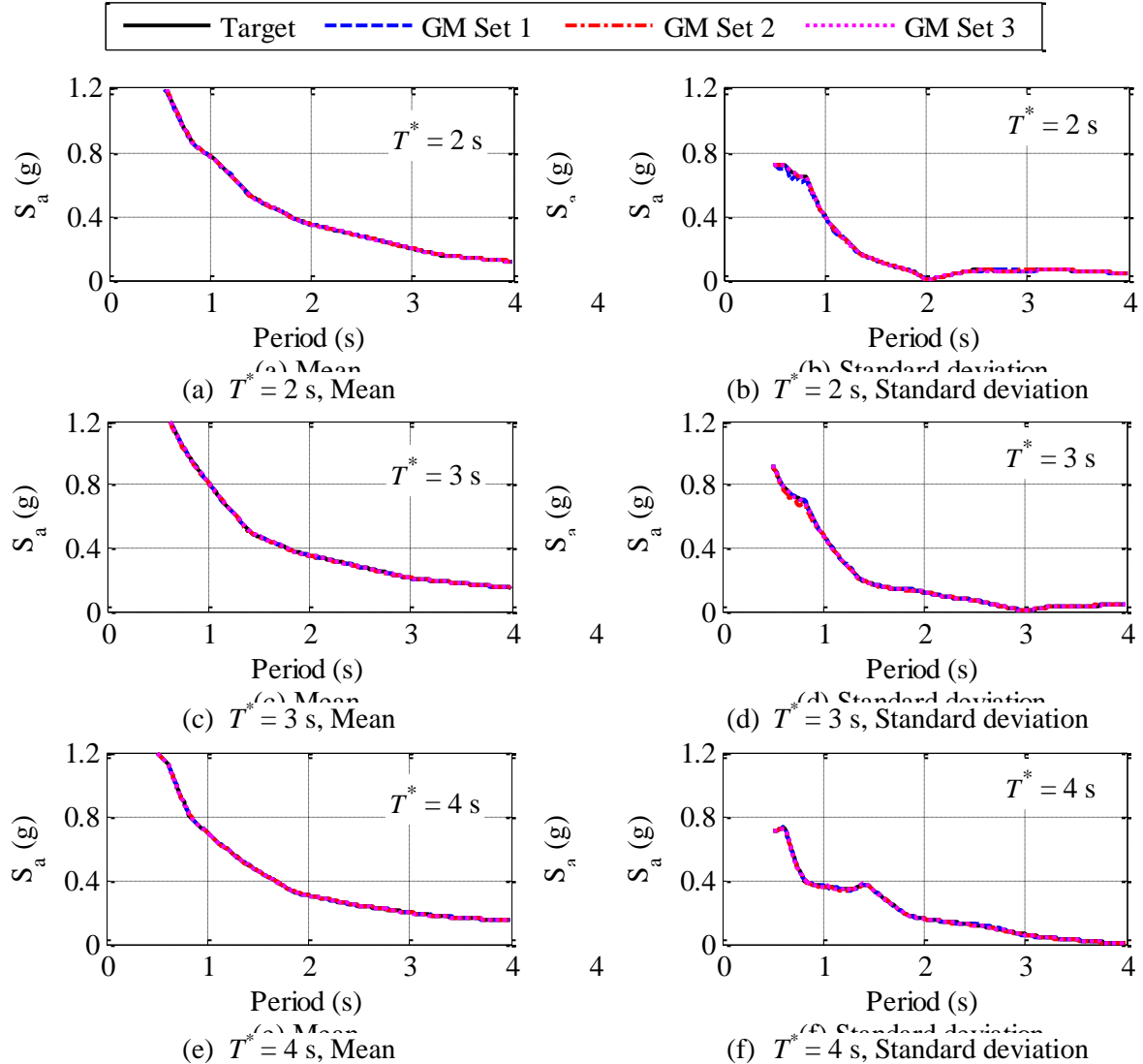


Fig. 10. Mean and standard deviation of target conditional spectra and spectra of spectrally matched motions in the X direction

6.5. Spectral displacements

Sections 6.1 through 6.4 present sets of 10,000-year ground motions consistent with the UHRS (1), UHRS-MaxMin (1), CMS with three conditioning periods (3), and CS with three conditioning periods (9). All 14 sets of 30 matched ground motions represent the 10,000-year seismic hazard at Diablo Canyon.

Fig. 10 presents the distributions of 5% damped spectral displacement of the 14 sets of 30 ground motions at different periods in the X direction. The *Max* component of the UHRS-MaxMin set is aligned in the horizontal X direction (see Table 1). The spectral displacements for a set of scaled ground motions are assumed to distribute lognormally at a given period.

Fig. 11(a) presents the distributions of spectral displacement in the X direction at a period, T , of 1.5 s for the ground motions spectrally matched to the 1) UHRS, 2) UHRS-MaxMin, 3) CMS with $T^* = 2$ s, and 4) CS with $T^* = 2$ s. The UHRS- (CMS-) scaled ground motions produce a median spectral displacement of 0.31 m (0.27 m) and differ from the corresponding 99th percentile spectral displacement by only 0.02 m (0.02 m). The UHRS-MaxMin-scaled ground motions produce a median (99th percentile) spectral displacement of 0.41 m (0.55 m). The spectral displacements of the three sets of 30 CS-scaled ground motions distribute in similar manner to one another since the ground motions are scaled to the same set of CS. The median (99th percentile) spectral displacement for each of the three sets of CS scaled ground motions is 0.26 m (0.49 m).

Fig. 11(b) presents the distributions of spectral displacement at $T = 2$ s with CMS and CS corresponding to $T^* = 2$ s. There is little difference in the distribution of the spectral displacements for the UHRS-, CMS- and CS-scaled ground motions, which is an expected result given the scaling procedures employed. A similar observation is made for Figs. 11(g) and 11(l), which present distributions of spectral displacement at periods of 3 s and 4 s, respectively, and for which $T = T^*$. The distributions of spectral displacements corresponding to the UHRS-MaxMin-scaled motions in these three panels follow pattern similar to that in Fig. 11(a).

For those cases where $T \neq T^*$ (panels other than (b), (g) and (l)), the trends are similar to Fig. 11(a), namely, 1) the spectral displacements of the UHRS-scaled motions are greater than those of the CMS-scaled motions, 2) the distributions of spectral displacement of the three sets of CS-scaled motions are similar, 3) the spectral displacements of the UHRS-scaled ground motions exceed those of the CS-scaled ground motions until approximately the 65th percentile, 4) the 84+th spectral displacements of the CS-scaled motions are significantly greater than those of the UHRS- and CMS-scaled motions, and 5) the spectral displacements for the ground motions consistent with UHRS-MaxMin exceed those for the other three spectra at percentiles below 90 and ordinates for the CS-scaled motions exceed those for UHRS-MaxMin-scaled motions at percentiles greater than 90 in some cases.

The distributions of spectral displacement in Y direction are identical to those in Fig. 11 (X direction), except for the UHRS-MaxMin-scaled ground motions because they were amplitude scaled with reciprocal (and smaller in almost all cases) factors (see Table 1).

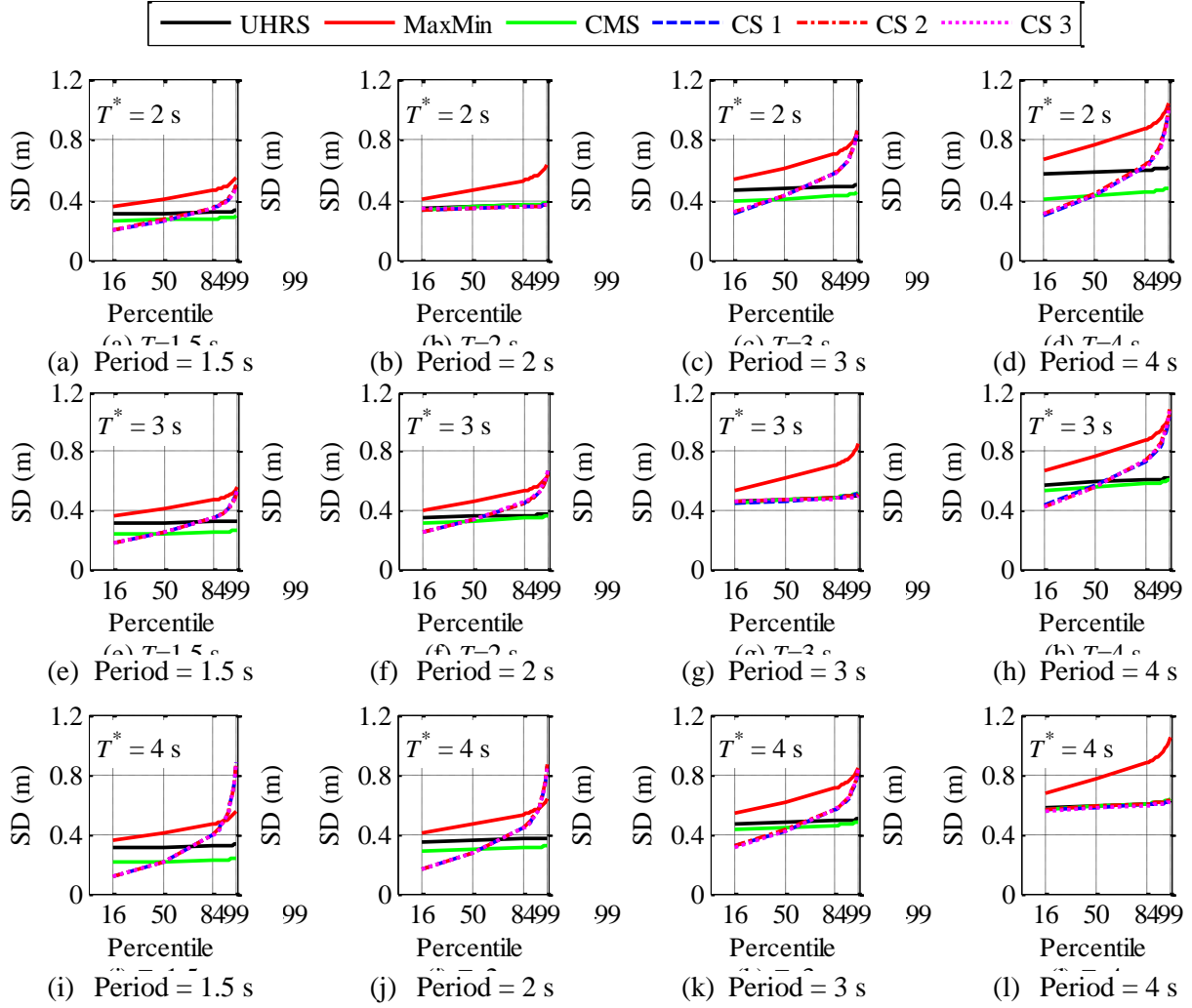


Fig. 11. Distributions of spectral displacement (SD) for the UHRS-, UHRS-MaxMin-, CMS-, and CS-scaled ground motions in the X direction at periods of 1.5 s, 2 s, 3 s and 4 s, and conditioning periods, T^* , of 2 s, 3 s, and 4 s for the CMS and CS

7. Ground motions consistent with 100,000-year response spectra

The 100,000-year UHRS (UHRS-MaxMin) ground motions are obtained by amplitude scaling the 10,000-year UHRS (UHRS-MaxMin) ground motions by a factor of 2.1 (see Section 5). The ground motions consistent with the 100,000-year CMS (CS) for the conditioning periods of 2 s, 3 s and 4 s are also obtained by amplitude scaling the corresponding 10,000-year CMS (CS) ground motions by a factor of 2.1 (see Section 5). The spectral displacements for the 100,000-year ground motions are obtained by amplitude scaling the spectral displacements for the 10,000-year ground motions by 2.1.

8. Response of the isolated nuclear power plant subjected to the 10,000- and 100,000-year ground motions

The lateral displacement of the center of mass at the basemat level of an NPP isolated using FP bearings can be estimated using a macro model (see [10]). Single FP bearings with a sliding period of 3 s (results for 4 s bearings are presented in [10]), reference coefficients of friction⁴ of 0.06 and 0.1⁵, static axial pressures of 10 MPa and 50 MPa, and friction at the sliding surface described using two friction models, namely, 1) Coulomb, and 2) a p - T - v model that accounts for the variations in the coefficient of friction with axial pressure on the bearing, sliding velocity, and temperature at the sliding surface during the course of earthquake shaking (see Kumar et al. [25]), are subjected to all of the ground motions of Sections 6 and 7, except for the CS-scaled motions with a conditioning period of 4 s⁶ (only some results for the 4 s CS-scaled motions are generated). The FP bearing is modeled using the *FPBearingPTV* element (see [10]) available with the open source software program OpenSees [26]. Mass proportional damping of 2% is assigned to the system, with the proportionality coefficient anchored to the sliding period of the bearing.

Fig. 12 presents the distributions of peak horizontal displacements⁷ of the FP bearings with axial pressure of 50 MPa and reference coefficient of friction of 0.1 subjected to the sets of 30 ground motions. Fig. 12(a) presents the results for the bearing subjected to the ground motions consistent with UHRS, UHRS-MaxMin, and CS and CMS with T^* of 2 s (Fig. 3(a)). The peak displacements for the UHRS-scaled motions are greater than the CMS- and CS-scaled motions at percentiles smaller than 80; the displacements for the CMS- and CS-scaled motions are comparable up to the 80th percentile. The displacements for the UHRS-MaxMin-scaled motions are greater than those for the other three representations of seismic hazard, at percentiles less than 95; the CS-displacements are the greatest at 95+ percentiles. The ratios of displacements for UHRS-MaxMin- (CMS-, CS-) to UHRS-scaled motions are 1.26 (0.73, 0.72), 1.34 (0.85, 1.15) and 1.42 (0.95⁸, 1.67) at 50th, 90th and 99th percentiles, respectively. Data for conditioning periods of 3 s and 4 s are presented in Figs. 12(b) and 12(c), respectively. The general trends are the same as those noted above for a conditioning period of 2 s. Fig. 13 presents the results for the 100,000-year shaking. The overall trends in the distributions of the peak displacements are similar. The 50th, 90th and 99th percentile displacements from Figs. 12 and 13 are compared in Fig. 14.

⁴ The coefficient of friction at the sliding surface measured at a reference axial pressure (usually static axial pressure), high sliding velocity (e.g., 1000 mm/s), and the ambient temperature of 20°C (see [10], [25] for further details).

⁵ The ground motions considered in this study impose significant displacement demand on the FP bearings, which dictates the choice of properties of FP bearings: sliding period and coefficient of friction.

⁶ The displacements of the FP bearings subjected to the 100,000-year CS-scaled motions with a conditioning period of 4 s exceed, for some ground motions, the radius of curvature of the bearing, leading to numerical problems.

⁷ The peak horizontal displacements of the isolation system subjected to a set of 30 ground motions are assumed to distribute lognormally (e.g., [10]).

⁸ The 99th percentile displacements for the CMS-scaled motions differ by only 5% from those for the UHRS-scaled motions, even though the CMS ordinates are considerably smaller than the UHRS ordinates at periods other than the conditioning period (see Fig. 10). This is explained by the higher dispersion in the CMS-displacements and that the displacements are assumed to distribute lognormally (e.g., [10]).

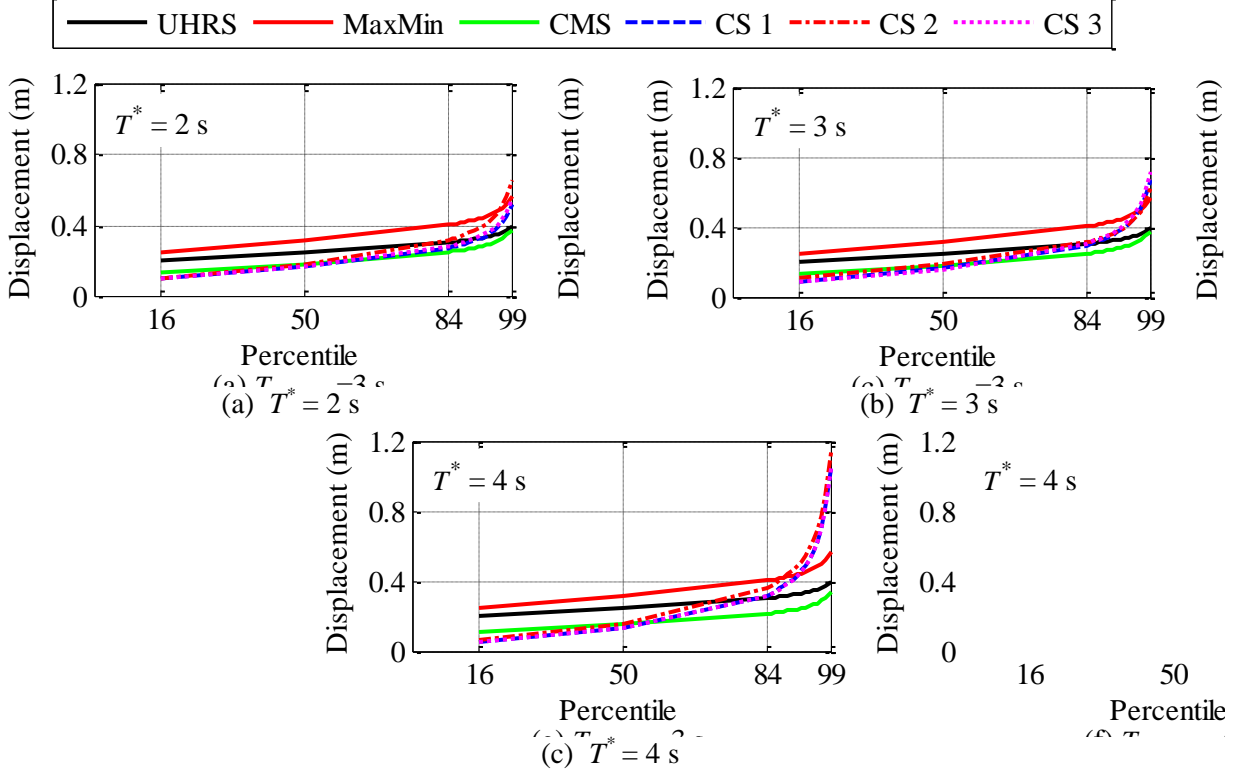


Fig. 12. Distributions of maximum displacement of FP bearings with a Coulomb-type coefficient of friction of 0.1 and a static axial pressure of 50 MPa subjected to ground motions consistent with different representations of 10,000-year shaking at the Diablo Canyon site

Fig. 14(a) presents the median responses of an FP bearing with a sliding period of 3 s subjected to ground motions consistent with 10,000-year UHRS, UHRS-MaxMin, CMS and CS. The median responses are greatest for the UHRS-MaxMin-scaled motions followed by the UHRS-scaled motions. The responses for CMS- and CS-scaled motions are comparable. The median responses for the 100,000-year ground motions presented in Fig. 14(b) follow a similar trend to the responses for the 10,000-year ground motions. Figs. 14(c) and 14(d) present the 90th percentile responses for 10,000-year and 100,000-year ground motions, respectively. The UHRS-MaxMin responses exceed those for the UHRS-scaled, and CMS- and CS-scaled motions with conditioning periods of 2 s and 3 s. The responses for the CS-scaled motions with a conditioning period of 4 s are comparable to those for the UHRS-MaxMin motions. Fig. 14(e) presents the 99th percentile responses for the 10,000-year ground motions. The responses for CS-scaled motions are considerably greater than those for the UHRS-MaxMin-scaled motions, especially for the conditioning period of 4 s. The responses for UHRS-scaled motions are virtually identical to those for the CMS-scaled motions.

Fig. 15 presents the data of Fig. 14 (except for the conditioning period of 4 s) when the friction at the sliding surface is defined using the p - T - v model⁹. The observations made on the

⁹ Temperature at the sliding surface influences the coefficient of friction, and consequently, the isolation system displacement, significantly, especially when the reference coefficient of friction and/or the static axial pressure on the bearing is high; effects of variation in axial pressure and sliding velocity during the earthquake shaking are rather small (see [10], [25]).

results presented in the Fig. 14 are also valid for Fig. 15. Results for other combinations of static axial pressure, reference coefficient of friction and friction models are presented in [10].

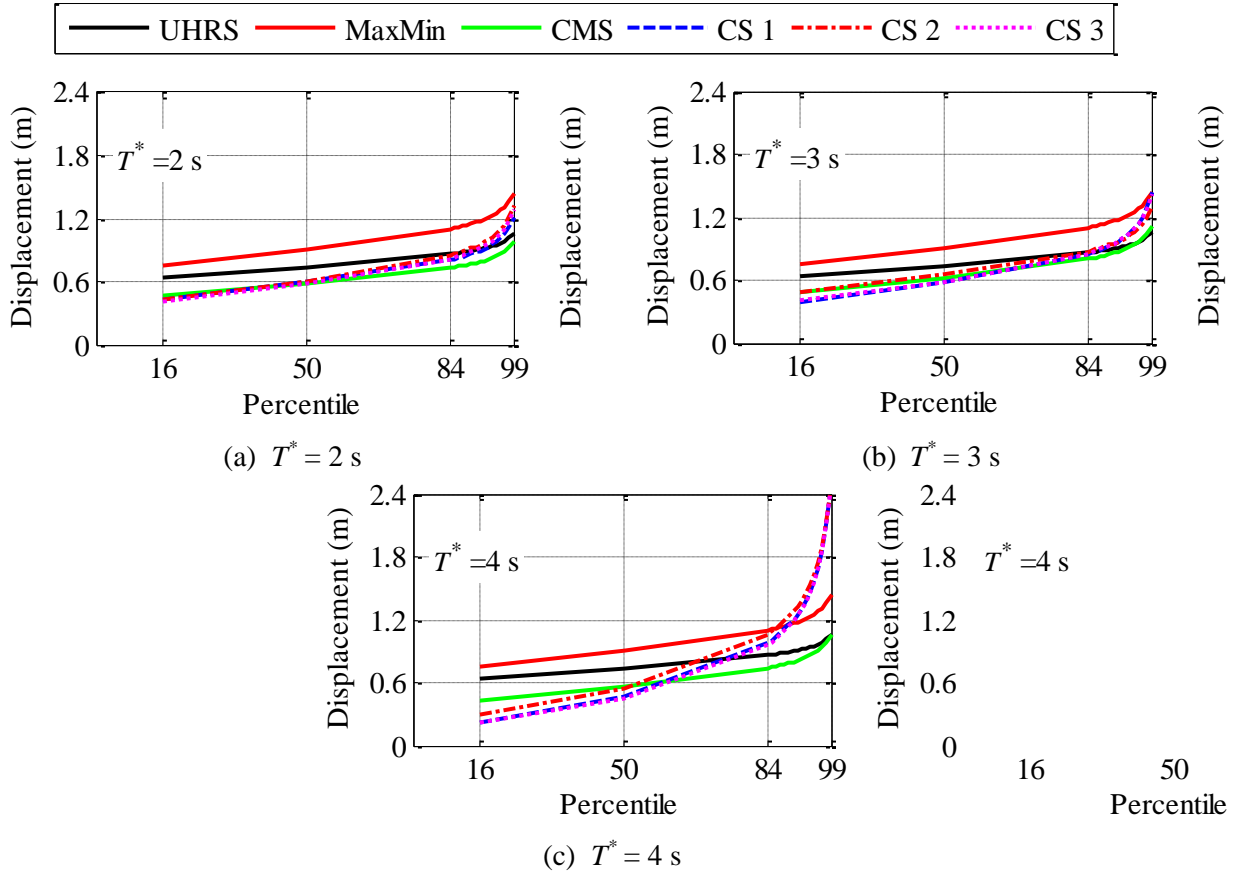


Fig. 13. Distributions of maximum displacement of FP bearings with a Coulomb-type coefficient of friction of 0.1 and a static axial pressure of 50 MPa subjected to ground motions consistent with different representations of 100,000-year shaking at the Diablo Canyon site

The general observations made previously are applicable irrespective of the axial pressure on the bearing, the choice of friction model, and/or hazard level. These observations were also found applicable to the results for the 4 s bearings with a subset of combinations of geometrical and material properties of the FP bearings considered in this paper (see [10]). The observations (including those for the 4 s FP bearing) are summarized below.

- i. The peak horizontal displacement responses of FP bearings are most significantly influenced by the choice of target spectra: UHRS, UHRS-MaxMin, CMS or CS.
- ii. Three sets of 30 ground motions were matched to each CS set. The choice of seed ground motions was found to have an insignificant effect on the response, compared with the choice of the target spectra.
- iii. The median peak horizontal displacements are greatest for the UHRS-MaxMin-scaled ground motions followed by UHRS-scaled motions. The median responses to the CMS- and CS-scaled motions are similar.
- iv. At the 90th percentile, the peak horizontal displacements for

- a. the CMS-scaled motions with conditioning periods of 2 s and 3 s differ by between 2% and 16% from those for the UHRS-scaled motions, and
- b. the UHRS-MaxMin-scaled motions are greater than those for other three representations of seismic hazard

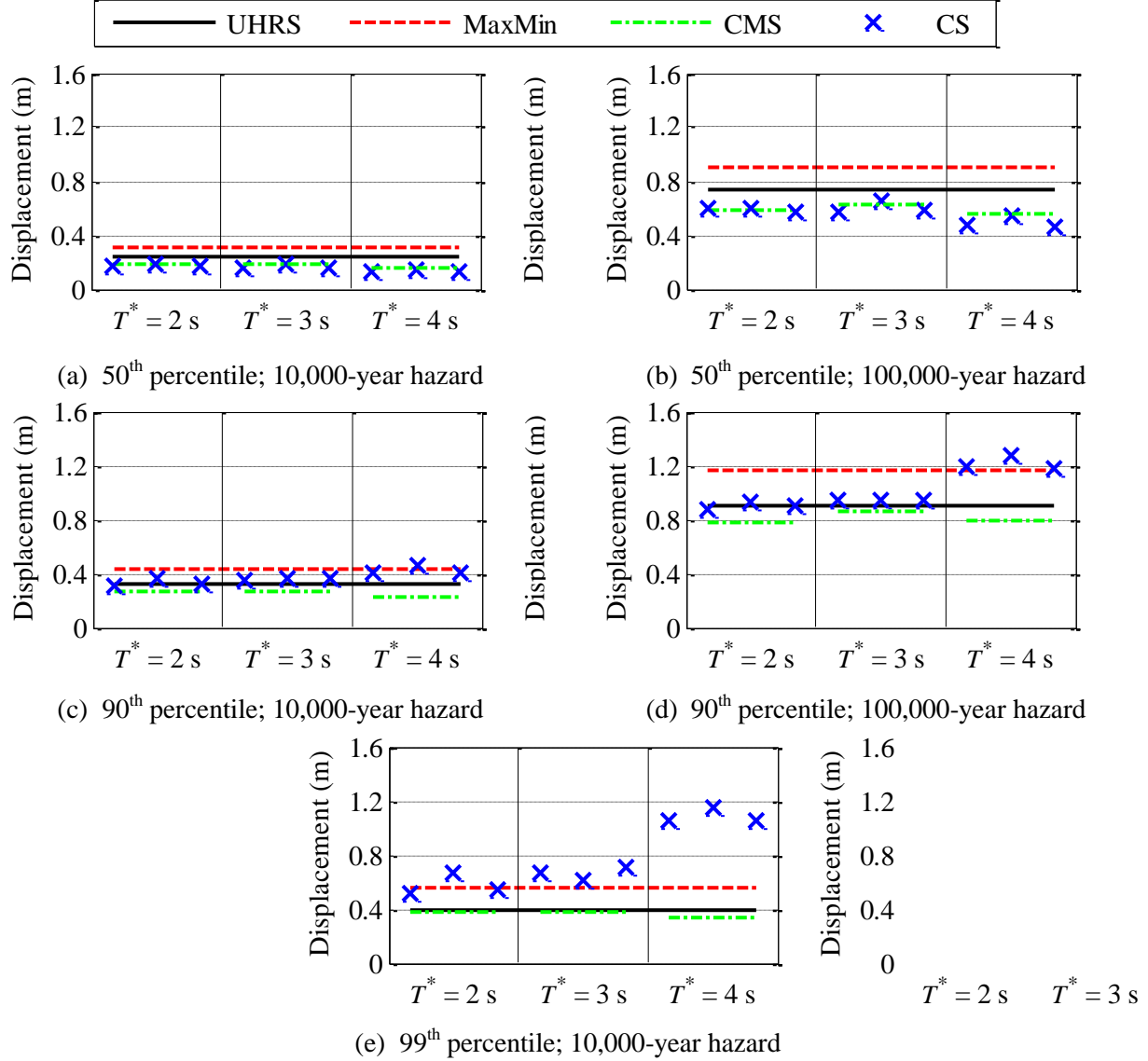


Fig. 14. Median, 90th and 99th percentile peak displacement responses of an FP bearing with a sliding period of 3 s, static axial pressure of 50 MPa, reference coefficient of friction of 0.1, and Coulomb friction model, subjected to 10,000-year and 100,000-year UHRS-, UHRS-MaxMin-, CMS- and CS-scaled ground motions

- v. At the 99th percentile, the peak horizontal displacement for 10,000-year shaking for
 - a. the CMS-displacements differ from those for the UHRS-displacements by up to 9%.
 - b. the UHRS-MaxMin motions are substantially greater than those for the UHRS- or CMS-scaled motions.

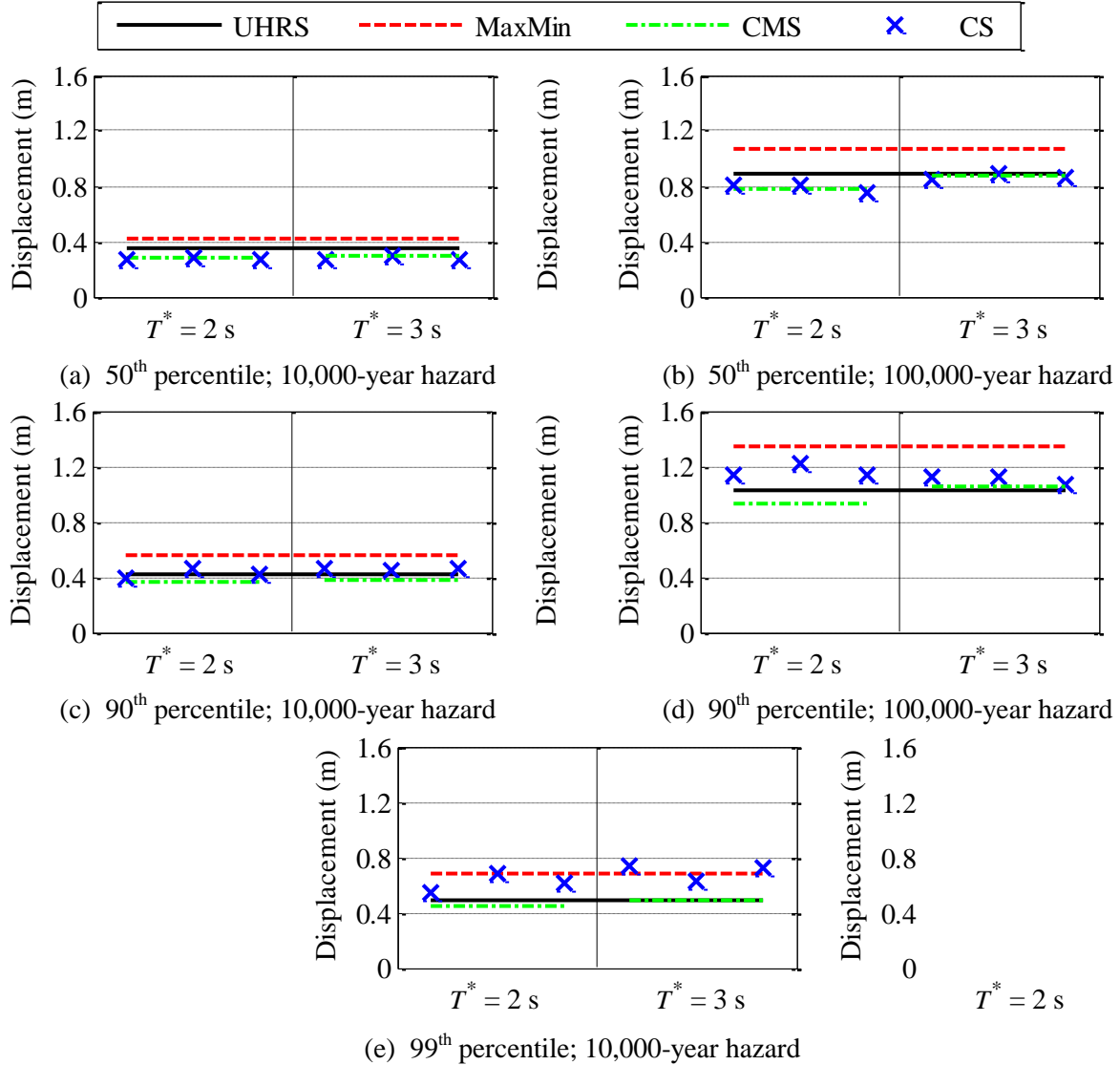


Fig. 15. Median, 90th and 99th percentile peak displacement responses of an FP bearing with a sliding period of 3 s, static axial pressure of 50 MPa, reference coefficient of friction of 0.1, and p - T - v friction model, subjected to 10,000-year and 100,000-year UHRS-, UHRS-MaxMin-, CMS- and CS-scaled ground motions

- vi. The 90th percentile peak horizontal displacement for 100,000-year shaking is greater than the 99th percentile peak horizontal displacement for 10,000-year shaking, for a given choice of target spectrum, and controls the design displacement capacity of the isolation system of an NPP.
- vii. The 90th percentile peak horizontal displacements for the UHRS-MaxMin-scaled motions are approximately 1.3 times those for the UHRS-scaled motions for both 10,000- and 100,000-year shaking.
- viii. The 90th percentile peak displacement of an FP bearing with friction defined using the p - T - v model subjected to the UHRS-MaxMin-motions is greater than that of an FP bearing with friction defined using the Coulomb model subjected to the UHRS-motions by a factor of between 1.4 and 1.7 (1.3 and 1.5) for 10,000-year (100,000-year) shaking,

for all combinations of static axial pressure and reference coefficient of friction. The factor increases with increases in static axial pressure from 10 MPa to 50 MPa and reference coefficient of friction from 0.06 to 0.1.

9. Conclusions

The following conclusions are drawn from the results of the response-history analyses performed on the macro model of an NPP isolated with single concave FP bearings, with a range of properties, subjected to ground motions consistent with return periods of 10,000 and 100,000 years at the site of Diablo Canyon Nuclear Generating Station:

- i. The UHRS should be used as the target spectrum with explicit consideration of the differences between the orthogonal horizontal components of the ground motions: UHRS-MaxMin ground motions.
- ii. An important design parameter for a seismic isolation system is the clearance to the hard stop, which is required to be greater than the 99th (90th) percentile peak displacement for 10,000-year (100,000-year) shaking. The 90th percentile peak displacement for the 100,000-year shaking is consistently greater than the 99th percentile peak displacement for the 10,000-year shaking, irrespective of the hazard definition. A smaller set of ground motions (e.g., 30) can be used to compute a 90th percentile displacement than would be needed to compute a 99th percentile displacement.
- iii. The 90th percentile peak displacement of an FP bearing with friction described using *p-T-v* model subjected to 100,000-year UHRS-MaxMin motions can be estimated by multiplying the median displacement of an FP bearing with friction described by the Coulomb model, subjected to the 10,000-year UHRS motions, by a factor of between 3.4 and 4.3, which depends on the static axial pressure and the reference coefficient of friction.

Recommendation (i) should not be seen as an endorsement of UHRS. Conditional mean spectra and conditional spectra are a more robust description of likely earthquake shaking but have not yet been extended to address a) highly nonlinear systems, which for an isolated NPP subjected to extreme earthquake shaking may include nonlinear behavior of the supporting soil, gapping and sliding at the soil-foundation interface, and the nonlinear isolators, and b) three components of earthquake input. For such systems, the optimal conditioning period will depend on the degree of inelastic response, which will vary by ground motion.

Acknowledgements

This research project was supported by a grant to MCEER and the University at Buffalo from the United States Nuclear Regulatory Commission and the Lawrence Berkeley National Laboratory (LBNL). This financial support is gratefully acknowledged. The authors thank Dr. Robert Budnitz of LBNL who advised the research team on technical matters and managed the project.

References

1. Huang, Y.-N., Whittaker, A. S. and Luco, N. (2008). Maximum spectral demands in the near-fault region. *Earthquake Spectra*, 24(1), 319-341.
2. Kammerer, A., Whittaker, A. S., and Constantinou, M. (forthcoming). Technical considerations for seismic isolation of nuclear facilities. Report NUREG-****, United States Nuclear Regulatory Commission, Washington, D.C.
3. Kammerer, A. M., Whittaker, A. S., and Coleman, J. (2016). Regulatory gaps and challenges for licensing advanced reactors using seismic isolation. Report INL/EXT-15-36945, Idaho National Laboratory, Idaho Falls, ID.
4. American Society of Civil Engineers (ASCE). (2016). Seismic analysis of safety-related nuclear structures and commentary. ASCE/SEI Standard 4-16, Reston, VA.
5. American Society of Civil Engineers (ASCE). (2005). Seismic design criteria for structures, systems and components in nuclear facilities. ASCE/SEI Standard 43-05, Reston, VA.
6. Baker, J. W., and Cornell, C. A. (2006). Spectral shape, epsilon and record selection. *Earthquake Engineering & Structural Dynamics*, 35(9), 1077-1095.
7. Jayaram, N., Lin, T., and Baker, J. W. (2011). A computationally efficient ground-motion selection algorithm for matching a target response spectrum mean and variance. *Earthquake Spectra*, 27(3), 797-815.
8. Huang, Y.-N., Yen, W.-Y., and Whittaker, A. S., (2017). Correlation of horizontal and vertical components of ground motion for response-history analysis of safety-related nuclear facilities. Submitted for re-review, Nuclear Engineering and Design.
9. Huang, Y.-N., Whittaker, A. S., Kennedy, R. P., and Mayes, R. L. (2009a). Assessment of base-isolated nuclear structures for design and beyond-design basis earthquake shaking. Report MCEER-09-0008, University at Buffalo, State University of New York, Buffalo, NY.
10. Kumar, M., Whittaker, A. S., and Constantinou, M. C. (2015a). Seismic isolation of nuclear power plants using sliding bearings. Report MCEER-15-0006, University at Buffalo, State University of New York, Buffalo, NY.
11. McGuire, R. K. (2004). Seismic hazard and risk analysis. Monograph MNO-10, Earthquake Engineering Research Institute, Oakland, CA.
12. American Society of Civil Engineers (ASCE). (2010). Minimum design loads for buildings and other structures. ASCE/SEI Standard 4-16, Reston, VA.
13. National Institute of Standards and Technology (NIST). (2011). Selecting and scaling earthquake ground motions for performing response-history analyses. NIST GCR 11-917-15, Gaithersburg, MD.
14. Federal Emergency Management Agency (FEMA). (2012). Seismic performance assessment of buildings, Volume 1: methodology. FEMA P-58-1, Washington, D.C.
15. Campbell, K. W., and Bozorgnia, Y. (2008). NGA ground motion model for the geometric mean horizontal component of PGA, PGV, PGD and 5% damped linear elastic response spectra for periods ranging from 0.01 to 10 s. *Earthquake Spectra*, 24(1), 139-171.
16. Hancock, J., Watson-Lamprey, J., Abrahamson, N., Bommer, J., Markatis, A., McCoy, E., and Mendis, R. (2006). An improved method of matching response spectra of

- recorded earthquake ground motion using wavelets. *Journal of Earthquake Engineering*, 10(SI 1), 67-89.
- 17. Al Atik, L. and Abrahamson, N. (2010). An improved method for nonstationary spectral matching. *Earthquake Spectra*, 26(3), 601-617.
 - 18. Boore, D. M., Watson-Lamprey, J., and Abrahamson, N. (2006). Orientation-independent measures of ground motion. *Bulletin of the Seismological Society of America*, 96(4A), 1502-1511.
 - 19. Beyer, K., and Bommer, J. J. (2006). Relationships between median values and between aleatory variabilities for different definitions of the horizontal component of motion. *Bulletin of the Seismological Society of America*, 96(4A), 1512-1522.
 - 20. Huang, Y.-N., Whittaker, A. S. and Luco, N. (2009b). Orientation of maximum spectral demand in the near-fault region. *Earthquake Spectra*, 25(3), 707-717.
 - 21. Gülerce, Z., and Abrahamson, N. A. (2011). Site-specific design spectra for vertical ground motion. *Earthquake Spectra*, 27(4), 1023-1047.
 - 22. Mosqueda, G., Whittaker, A. S., and Fenves, G. L. (2004). Characterization and modeling of Friction Pendulum bearings subjected to multiple components of excitation. *Journal of Structural Engineering*, 130(3), 433-442.
 - 23. Huang, Y.-N., Whittaker, A. S., and Luco, N. (2010). Seismic performance assessment of base-isolated safety-related nuclear structures. *Earthquake Engineering and Structural Dynamics*, 39(13), 1421-1442.
 - 24. Baker, J. W., and Jayaram, N. (2008). Correlation of spectral acceleration values from NGA ground motion models. *Earthquake Spectra*, 24(1), 299-317.
 - 25. Kumar, M., Whittaker, A. S., and Constantinou, M. C. (2015b). Characterizing friction in sliding isolation bearings. *Earthquake Engineering & Structural Dynamics*, 44(9), 1409-1425.
 - 26. Pacific Earthquake Engineering Research Center (PEER). (2015). Open System for Earthquake Engineering Simulation (Version 2.4.6) [Computer program], Berkeley, CA.

- Four alternate representations of seismic hazard considered: UHRS, CMS, CS and UHRS-*MaxMin*
- Fourteen sets of 30 ground motions consistent with the four hazard definitions and two levels of shaking developed for a hypothetical site of seismically isolated nuclear power plant (NPP)
- Seismic hazard definition affects the displacements most significantly; effect of seed motions appears to be small
- For a given hazard definition, the isolation-system displacement capacity is controlled by the 90th percentile displacement under 100,000-year shaking (beyond design basis shaking)
- Seismic hazard should be defined in terms of UHRS with explicit considerations for the differences between orthogonal components (UHRS-*MaxMin*)
- Temperature-dependence of coefficient of friction at the sliding surface of a sliding bearing should be accounted for in the analysis